Am J Physiol Regul Integr Comp Physiol 312: R1017–R1028, 2017.
First published April 24, 2017; doi:10.1152/ajpregu.00032.2017.

RESEARCH ARTICLE | *Physical Activity and Inactivity*

Improved skeletal muscle Ca^{2+} regulation in vivo following contractions in mice overexpressing PGC-1α

Hiroaki Eshima,[1] Shinji Miura,[2] Nanami Senoo,[2] Koji Hatakeyama,[1] David C. Poole,[3] and Yutaka Kano[1]

[1]*Department of Engineering Science, Bioscience and Technology Program, University of Electro-Communications, Tokyo, Japan;* [2]*Laboratory of Nutritional Biochemistry, Graduate School of Nutritional and Environmental Sciences, University of Shizuoka, Shizuoka, Japan; and* [3]*Departments of Anatomy and Physiology and Kinesiology, Kansas State University, Manhattan, Kansas*

Submitted 31 January 2017; accepted in final form 12 April 2017

Eshima H, Miura S, Senoo N, Hatakeyama K, Poole DC, Kano Y. Improved skeletal muscle Ca^{2+} regulation in vivo following contractions in mice overexpressing PGC-1α. *Am J Physiol Regul Integr Comp Physiol* 312: R1017–R1028, 2017. First published April 24, 2017; doi:10.1152/ajpregu.00032.2017.—In skeletal muscle, resting intracellular Ca^{2+} concentration ($[Ca^{2+}]_i$) homeostasis is exquisitely regulated by Ca^{2+} transport across the sarcolemmal, mitochondrial, and sarcoplasmic reticulum (SR) membranes. Of these three systems, the relative importance of the mitochondria in $[Ca^{2+}]_i$ regulation remains poorly understood in in vivo skeletal muscle. We tested the hypothesis that the capacity for Ca^{2+} uptake by mitochondria is a primary factor in determining $[Ca^{2+}]_i$ regulation in muscle at rest and following contractions. Tibialis anterior muscle of anesthetized peroxisome proliferator-activated receptor-γ coactivator-1α (PGC-1α)-overexpressing (OE, increased mitochondria model) and wild-type (WT) littermate mice was exteriorized in vivo and loaded with the fluorescent probe fura 2-AM, and Rhod 2-AM Ca^{2+} buffering and mitochondrial $[Ca^{2+}]$ were evaluated at rest and during recovery from fatiguing tetanic contractions induced by electrical stimulation (120 s, 100 Hz). In addition, the effects of pharmacological inhibition of SR (thapsigargin) and mitochondrial [carbonyl cyanide-*4*-(trifluoromethoxy) phenylhydrazone (FCCP)] function were examined at rest. $[Ca^{2+}]_i$ in WT remained elevated for the entire postcontraction recovery period (+6 ± 1% at 450 s), but in PGC-1α OE $[Ca^{2+}]_i$ returned to resting baseline within 150 s. Thapsigargin immediately and substantially increased resting $[Ca^{2+}]_i$ in WT, whereas in PGC-1α OE this effect was delayed and markedly diminished (WT, +12 ± 3; PGC-1α OE, +1 ± 2% at 600 s after thapsigargin treatment, $P < 0.05$). FCCP abolished this improvement of $[Ca^{2+}]_i$ regulation in PGC-1α OE. Mitochondrial $[Ca^{2+}]$ accumulation was observed in PGC-1α OE following contractions and thapsigargin treatment. In the SR, PGC-1α OE downregulated SR Ca^{2+}-ATPase 1 (Ca^{2+} uptake) and parvalbumin (Ca^{2+} buffering) protein levels, whereas mitochondrial Ca^{2+} uptake-related proteins (Mfn1, Mfn2, and mitochondrial Ca^{2+} uniporter) were upregulated. These data demonstrate a heretofore unappreciated role for skeletal muscle mitochondria in $[Ca^{2+}]_i$ regulation in vivo following fatiguing tetanic contractions and at rest.

calcium homeostasis; mitochondrial calcium sequestration; thapsigargin

PRECISE SPATIAL AND TEMPORAL control of ATP and Ca^{2+} is requisite for skeletal muscle contractile function, and their availability is regulated by two major intracellular organelles, sarcoplasmic reticulum (SR) and mitochondria. Accordingly, the rate of muscle contraction-relaxation cycling is widely believed to be dependent on the capacity for Ca^{2+} release-reuptake of the SR (2, 7). In parallel with this SR function, it has been demonstrated in in vitro muscle that mitochondrial $[Ca^{2+}]$ increases during/after tetanic contractions, supporting that these organelles also play a role in regulating intracellular Ca^{2+} ($[Ca^{2+}]_i$) (6, 10, 39, 41). However, the precise mitochondrial contribution to skeletal muscle Ca^{2+} handling during the normal physiological state remains to be defined.

Isolated single or skinned muscle fibers (i.e., in vitro) are bereft of vascular circulation and are usually sustained in nonphysiologically high O_2 environments that impact intramyocyte energetics and redox regulation as well as mitochondrial function. Recently, we succeeded in measuring $[Ca^{2+}]_i$ in vivo within rat skeletal muscle following repeated tetanic contractions (18, 20, 42, 43). Using this approach, we investigated the mechanistic bases for impaired Ca^{2+} handling (Ca^{2+} release and reuptake by SR) in streptozotocin diabetic skeletal muscle in vivo and determined its independence from SR Ca^{2+}-ATPase protein content (19, 20). Because diabetic muscle evinces a reduced mitochondrial enzyme activity (20, 24), we proposed that mitochondrial, rather than SR, dysfunction might contribute to the impaired $[Ca^{2+}]_i$ regulation in streptozotocin diabetes. That notion is supported by the finding that, in healthy mammalian muscle in vivo, physiologically stimulated cytosolic Ca^{2+} transients elevate mitochondrial Ca^{2+} levels (40). That this event tracks the cytosolic Ca^{2+} rise, but occurs several milliseconds later, adds further weight to the contention that mitochondria are involved directly in muscle Ca^{2+} homeostasis. Notwithstanding the above, the overall importance of mitochondrial $[Ca^{2+}]$ removal in healthy muscle under in vivo conditions remains poorly understood.

Peroxisome proliferator-activated receptor-γ coactivator-1α (PGC-1α) is a key regulator of mitochondrial function, oxidative metabolism, and energy homeostasis in a variety of tissues (30). Crucially, for the present investigation, in skeletal muscle PGC-1α upregulates mitochondrial biogenesis while promoting a fiber-type transformation toward more oxidative fibers by increasing muscle oxidative potential and microvascular transport capacity (3, 36, 48). We have previously demonstrated that overexpression of PGC-1α in fast-twitch muscles in-

Address for reprint requests and other correspondence: Y. Kano, Dept. of Engineering Science, Bioscience and Technology Program, University of Electro-Communications Chofu, Tokyo 1828585, Japan (e-mail: kano@pc.uec.ac.jp).

creases mitochondrial volume density and function, which translates to improved endurance performance (25, 44).

In the present investigation we tested the overarching hypothesis that the capacity for mitochondrial Ca^{2+} uptake constitutes a primary determinant of $[Ca^{2+}]_i$ regulation at rest and following muscle contractions. Specifically, by elevating mitochondrial content and function using a genetic model of PGC-1α overexpression (PGC-1α OE) we predicted that $[Ca^{2+}]_i$ control will be improved. For instance, when SR function (i.e., Ca^{2+} sequestration) is noncompetitively inhibited by the sesquiterpene lactone thapsigargin, $[Ca^{2+}]_i$ control will be substantially maintained by mitochondrial Ca^{2+} removal (better in PGC-1α OE muscles), which would subsequently be removed by carbonyl cyanide-*4*-(trifluoromethoxy) phenylhydrazone (FCCP)-induced uncoupling of mitochondrial function.

METHODS

Ethical Approval

All experiments were conducted under the guidelines established by the Physiological Society of Japan and were approved by The University of Electro-Communications Institutional Animal Care and Use Committee.

Animals

Transgenic mice were produced overexpressing PGC-1α-b in skeletal muscle (hereafter, PGC-1α OE mice, 2–5 mo of age) as previously described (25, 34, 44). Briefly, human skeletal muscle-α actin promoter provided by Drs. E. C. Hardeman and K. L. Guven (Children's Medical Research Institute, Westmead, Australia) was used to express PGC-1α isoform in skeletal muscle. PGC-1α mice (heterozygotes, BDF 1 background) and wild-type (WT) C57BL6 mice were crossed, and the offspring (heterozygote and WTe, born in the same time period) were used for the experiments. The copy number of PGC-1α transgene in transgenic mice was estimated as described previously (35). We used the B line of PGC-1α mice in this study; two independent lines of PGC-1α mice showed similar phenotypes. The PGC-1α data in this model have been reported previously (44). Mice were maintained on a 12:12-h light-dark cycle and received food and water ad libitum. The mice were anesthetized using pentobarbital sodium (60 mg/kg ip), and supplemental doses of anesthesia were administered as needed. At the end of experimental protocols, animals were killed by pentobarbital sodium overdose.

Muscle Preparation

For all experimental techniques, the tibialis anterior (TA) muscle was used. This muscle is composed primarily of fast-twitch fibers (8). We applied our previous method developed in the rat to the mouse TA muscle (18). Briefly, the TA muscle was resected at the distal tendon and gently exteriorized with minimal blood loss and tissue/microcirculatory damage with the feed vascular and nervous supplies remaining intact. The exposed muscle tissue was kept moist by superfusing with warmed Krebs-Henseleit buffer (KHB; in mM: 132 NaCl, 4.7 KCl, 21.8 $NaHCO_3$, 2 $MgSO_4$, and 2 $CaCl_2$) equilibrated with 95% N_2-5% CO_2 and adjusted to pH 7.4, at 37°C.

Experimental Protocols

Intracellular Ca^{2+} measurement. Intracellular Ca^{2+} measurements were performed, as described previously (18). The fluorescent Ca^{2+} indicator fura 2-AM (5 mM; Dojindo Laboratories, Kumamoto, Japan) was dissolved in DMSO and Pluronic F-127 and dispersed in KHB solution at a final concentration of 40 μM. The muscles were incubated in fura 2-AM/KHB solution for 60 min on a 37°C hotplate. After incubation, muscles were rinsed with dye-free KHB solution to remove nonloaded fura 2 and observed by fluorescence microscopy using a ×4 objective lens (0.20 numerical aperture; Nikon, Tokyo, Japan) on the 37°C glass hotplate (Kitazato Supply, Shizuoka, Japan). Thereafter, 340- and 380-nm wavelength excitation light was delivered using a Xenon lamp equipped with appropriate fluorescent filters, and pairs of fluorescence images were captured through the 510-nm emission wavelength filter for ratiometry. Fluorescence images were captured by a high-sensitivity charge-coupled device digital camera (ORCA-Flash 2.8; Hamamatsu Photonics, Hamamatsu, Japan) using image-capture software (NIS-Elements Advanced Research; Nikon). The scan requirements were set at 0.5–1 s/image, over a 1,750 × 1,310-μm (1.82 pixel/μm) imaging field of view. This resulted in a time frame between 1 and 2 s. The fluorescence intensity of serial ratio images was normalized to the starting point (i.e., precondition, R_0) of each experiment (R/R_0). Pilot studies confirmed that the 340-to-380-nm ratio value (i.e., resting $[Ca^{2+}]_i$) was unchanged over the 90-min observation period ($n = 6$). This contrasted with the in vitro state (surgically isolated) where $[Ca^{2+}]_i$ progressively increased ($n = 5$).

Mitochondrial $[Ca^{2+}]$ measurement. Mitochondrial $[Ca^{2+}]$ measurements were performed, as described previously (1, 6, 10). Rhod 2-AM has a rhodamine-like fluorophore whose excitation and emission maxima are 557 and 581 nm, respectively. Briefly, the muscles were incubated in 50 μM Rhod 2-AM/KHB solution for 60 min on a 37°C hotplate. After incubation, muscles were rinsed with dye-free KHB solution to remove nonloaded Rhod 2-AM and observed by fluorescence microscopy using a ×4 objective lens on the 37°C glass hotplate. The fluorescence intensity of serial fluorescence images was normalized to the starting point (i.e., precondition, F_0) of each experiment (F/F_0).

Stimulation: Experiment 1

The contraction protocols have been detailed previously (18). Briefly, cuff electrodes were mounted on the peroneal nerves. After a 10- to 15-min postsurgery stabilization period, TA tetanic muscle contractions (100 Hz frequency, 4–8 V, no interval) were elicited by electrical stimulation (SEN-8203; Nihon Kohden, Tokyo, Japan) for 2 min. This contraction paradigm was designed to produce maximum force and significant fatigue, which simulates how muscles might be required to contract isometrically under physiological conditions. Specifically, it was important to use a contraction paradigm that produced significant fatigue and did not depart substantially from how muscle(s) might contract physiologically. This 2-min isometric contraction is akin to someone gripping the handles of their suitcase while they walked a short distance, perhaps stand on tip toe in a crowd to get a better view of a sporting event, or remaining crouched while downhill skiing, etc. To measure force, the distal tendon of TA muscles was isolated and connected by fine wire to a strain gauge. Torque was monitored by computer using Power Laboratory/4s (AD Instruments, Colorado Springs, CO) via a strain gauge-linked motor device (0–10 mN/m, full-scale deflection, model no. RU-72; NEC Medical Systems, Tokyo, Japan) during all contraction protocols. The muscle force during electrical stimulation was resolved as active force and plotted graphically as an index of fatigue over the 2-min contraction period.

Pharmacological Agents: Experiment 2

Pharmacological agents thapsigargin and FCCP were purchased from Sigma-Aldrich (St. Louis, MO). Thapsigargin is an irreversible SR Ca^{2+}-ATPase (SERCA) inhibitor that induces Ca^{2+} release from SR (16, 23). FCCP acts as an oxidative phosphorylation uncoupler in mitochondria that effectively blocks mitochondrial Ca^{2+} uptake (10, 29). Thapsigargin (10 mM) was prepared fresh daily in dimethyl sulfoxide (DMSO) (23), and a stock solution of FCCP (10 mM) was prepared in ethanol and used during the subsequent month as described previously

(10). After fura 2 incubation and rinse, FCCP was applied for 5 min before the start of experiments. Before the start of experiments, thapsigargin and FCCP, independently or together depending on the protocol, were dissolved in KHB solution at a final concentration of 100 and 10 μM, respectively. All experiments were performed at room temperature, and the muscles were mounted on the 37°C glass hotplate.

Histology

At the end of the experiments, TA muscles were resected under anesthesia, and blocks were frozen rapidly in isopentane cooled in liquid nitrogen. Serial 10-μm sections were made with a cryostat (CM1510; Leica, Tokyo, Japan) at −20°C and mounted on poly-lysine-coated slides. Whole sections were stained for hematoxylin and eosin, succinate dehydrogenase (SDH), and fast myosin heavy chain (MHC). The SDH activities in individual muscle fibers in histological sections were examined and analyzed as described previously (18, 20). Mouse fast MHC monoclonal antibody isoforms were used; these react specifically with type IIa (1:1,000; SC-71) and IIx (1:100; BF-35) MHCs. These were supplied by Developmental Studies Hybridoma Bank (University of Iowa). A M.O.M. Immunodetection Kit (Vector Laboratories, Burlingame, CA) was used to reveal the immunohistochemical reaction according to the manufacturer's instructions. Thereafter, a Vectastain ABC kit (Vector Laboratories) and diaminobenzidine tetrahydrochloride were used as a chromogen to localize peroxidase in the secondary antibody. In photographs of serial sections, type IIa and type IIx stained muscle fibers were identified, and type IIb nonstained fibers were considered to be type IIb fibers. The cross-sectional areas and SDH activities were measured by tracing fiber outlines of ~322 fibers from muscle sections. The images were digitized as gray-level pictures. Each pixel was quantified as one of 256 gray levels and then automatically converted to optical density using ImageJ software.

Western Blotting Analysis

Critical proteins involved in skeletal muscle Ca^{2+} regulation were determined by Western blotting analysis. SR Ca^{2+}-related proteins {ryanodine receptor [RyR (Ca^{2+} release)], SERCA1 (Ca^{2+} uptake), and CSQ (Ca^{2+}-binding protein of SR)}, a small cytosolic Ca^{2+}-binding protein [parvalbumin (PV)], and mitochondrial Ca^{2+}-related proteins {Mfn1 and Mfn2 (mitochondria-associated SR membranes), mitochondrial Ca^{2+} uniporter (MCU, the inner mitochondrial membrane), and cytochrome *c* oxidase subunit 4 [Cox IV (marker of loading control for mitochondria)]} were detected. Western blotting was performed as described previously (44). TA muscles were removed and homogenized in RIPA Lysis Buffer (Upstate Biotechnology, Lake Placid, NY) containing 1 mM sodium orthovanadate, 1 mM sodium fluoride, and the "Complete Mini, EDTA-free" protease inhibitor cocktail (1 tablet/10 ml). Homogenates were centrifuged at 14,000 rpm for 30 min at 4°C. Supernatant proteins were then quantified using the BCA protein assay kit (Thermo Scientific, West Palm Beach, FL). The sample (10 μg total protein/lane) were separated on 4–12.5% polyacrylamide gels at 150 volts and then transferred to Amersham Hybond-P membranes (GE Healthcare, Buckinghamshire, UK) for 60 or 100 min at 72 mA using the semidry method. After transfer, the membranes were blocked with Blocking One or 1–3% skim milk at room temperature for 1 h. After blocking the membranes were then incubated with primary antibodies [anti-RyR, 34C antibody, 1:5,000 (Thermo Scientific); anti-CSQ, VIIID12 antibody, 1:1,000 (Thermo Scientific); anti-SERCA1, IIH11 antibody, 1:2,500 (Thermo Scientific); α-Mfn1, 1:1,000, ab57602 (abcam); α-Mfn2, 1:1,000, ab56889 (abcam); anti-MCU, HPA016480, 1:1,000 (atlas); anti-parvalbumin, ab32895 antibody, 1:1,000 (abcam); and anti-Cox IV, ab14744 antibody, 1:1,000 (abcam)] overnight at 4°C. Subsequently, the membranes were added to goat anti-mouse IgG linked to peroxidase (SC-2055; Santa Cruz Biotechnology, Santa Cruz, CA) and incubated for 1 h at room temperature. The bound antibodies were detected by Chemi-Lumi One Super Kit (Nacalai Tesque) and analyzed with ImageQuant LAS-4000 (GE Healthcare Life Sciences, Tokyo, Japan). Protein levels were expressed relative to the WT samples and normalized to α-tubulin antibody (1:1,000, GT114; GeneTex, Irvine, CA).

Electron Microscopy

Preparation of samples and quantitative analysis for electron microscopy. For transmission electron microscopy, [tissues] were fixed with 2.5% glutaraldehyde (TAAB) in 0.1 M phosphate buffer (pH 7.4), followed by postfixation with 1% OsO_4 in the same buffer. Fixed specimens were dehydrated with a graded series of ethanol and embedded in Epok 812 (Oken shoji, Tokyo, Japan). Ultrathin sections were cut and stained with uranyl acetate and lead citrate. Specimens were examined with an HT7700 transmission electron microscope (Hitachi, Tokyo, Japan). Next, electron micrographs were taken at high magnification using the Soft Imaging System. Individual mitochondria from three WT and PGC-1α OE mice were manually traced in longitudinal orientations using ImageJ software. Total number of mitochondrial and individual mitochondria area measurements, and the closest distance between sites of Ca^{2+} release from SR and mitochondrial outer membrane, was measured. The distance between sites of Ca^{2+} release from the SR and mitochondrial outer membrane have been reported previously (9, 39).

Table 1. *Characteristics of muscle morphology and oxidative enzyme activity in WT and PGC1-α OE mice*

	Superficial Region		Deep Region	
	WT	PGC1-α OE	WT	PGC1-α OE
Muscle composition, %				
Type IIa	4.8 ± 1.3	6.4 ± 2.3	26.7 ± 2.8	31.6 ± 3.8
Type IIx	24.6 ± 2.2	59.5 ± 4.2**	42.1 ± 4.8	55.4 ± 3.2
Type IIb	70.5 ± 2.1	34.1 ± 5.8**	31.1 ± 4.0	12.9 ± 1.2*
Cross-sectional area, μm^2				
Type IIa	1,338.0 ± 234.0	1,773.4 ± 156.8	1,195.2 ± 125.7	1,467.8 ± 106.4
Type IIx	1,673.9 ± 133.5	2,412.9 ± 228.2*	1,745.0 ± 154.2	2,046.7 ± 224.1
Type IIb	2,680.5 ± 155.3	2,897.2 ± 199.4	2,464.6 ± 170.6	1,825.9 ± 198.0
Total	2,359.6 ± 145.6	2,525.1 ± 165.1	1,821.5 ± 133.8	1,831.4 ± 177.1
SDH activity, OD				
Type IIa	178.8 ± 9.1	185.2 ± 4.0	165.1 ± 8.7	153.5 ± 5.4
Type IIx	170.4 ± 8.5	165.9 ± 5.1	145.4 ± 4.8	144.3 ± 4.9
Type IIb	86.4 ± 3.1	121.2 ± 4.0**	79.8 ± 5.4	136.3 ± 4.5
Total	111.9 ± 4.4	150.4 ± 2.9**	130.9 ± 6.3	146.0 ± 4.9

Values are means ± SE; $n = 5$ mice. WT, wild type; PGC1-α OE, peroxisome proliferator activated receptor-γ coactivator-1-overexpressing mice; SDH, succinate dehydrogenase; OD, optical density. Significant difference between WT and PGC1-α. *$P < 0.05$. **$P < 0.01$.

Statistical Analysis

Values are expressed as means ± SE. Statistical analyses were performed in Prism version 7.0 (GraphPad Software, San Diego, CA). The changes in $[Ca^{2+}]_i$ levels and muscle force from resting or initial levels were compared within groups using a two-way ANOVA with repeated measures followed by Dunnet's post hoc test. The comparisons between groups were analyzed using a two-way ANOVA with repeated measures followed by post hoc comparisons of the group means using the Tukey's multiple-comparison test. Unpaired *t*-tests (2-tailed) were used for relative protein levels, histological data, and electron microscopy data. The level of significance was set at $P < 0.05$.

RESULTS

Animal and Muscle Data

Neither body (WT, 23.3 ± 0.7; PGC-1α OE, 24.0 ± 0.6 g; $P > 0.05$) nor TA (WT, 49.0 ± 0.4; PGC-1α OE, 48.6 ± 1.1 mg; $P > 0.05$) mass was different between WT and PGC-1α OE mice.

Histological evaluation. Table 1 shows muscle morphology and oxidative enzyme activity (SDH) in the TA superficial and deep regions of WT and PGC-1α OE mice. A muscle fiber type shift from myosin heavy chain (MHC) IIb (fast-twitch glycolytic fibers) to MHC IIx (mouse fast-twitch oxidative fibers) was found in both TA regions of PGC-1α OE compared with WT mice but was especially prominent in the superficial region. Total SDH activity increased significantly in PGC-1α OE in both superficial (+34.4% vs. WT) and deep (+11.5% vs. WT) TA regions. This effect was driven exclusively by the elevated IIb SDH activity and occurred despite their reduced contribution to TA mass. With the exception of a hypertrophic response in the superficial IIx fibers, muscle fiber cross-sectional area was not different between WT and PGC-1α OE.

Intramyocellular Ca^{2+} and Muscle Force Production Following 120-s Tetanic Contractions

In vivo $[Ca^{2+}]_i$ at resting baseline and following the 120-s tetanic muscle contraction (*experiment 1*) is shown in Fig. 1, *left* (photomicrographs) and *right* (temporal profiles). $[Ca^{2+}]_i$ peak values were increased to a similar level in WT and PGC-1α OE (WT, 16 ± 1; PGC-1α OE, 20 ± 2%, $P > 0.05$;

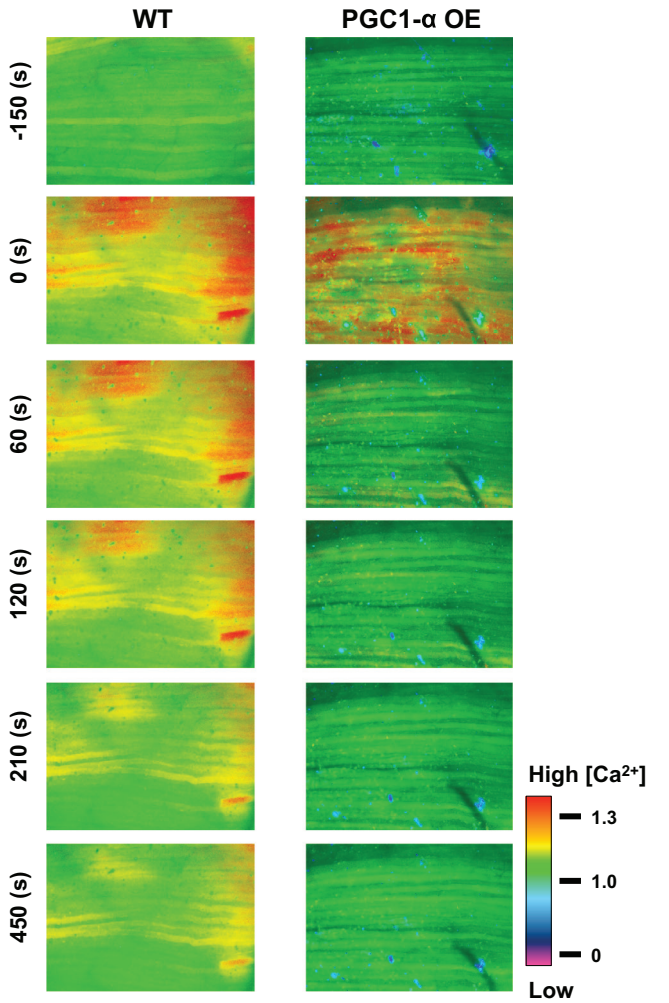

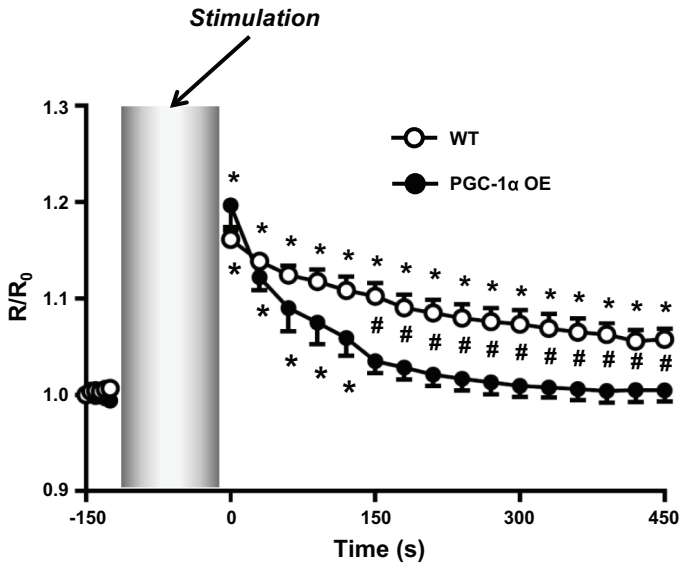

Fig. 1. In vivo intracellular Ca^{2+} concentration ($[Ca^{2+}]_i$) profiles following 120-s contractions for tibialis anterior muscles from wild-type (WT) and peroxisome proliferator-activated receptor-γ coactivator-1α (PGC-1α)-overexpressing (OE) mice. *Left*, fura 2-AM fluorescence images were captured continuously with no delay following contraction. Scale bar = 200 μm. *Right*, fluorescence was measured before contraction and continuously for 450 s of recovery, and ratiometrically quantified data were graphed as changes from baseline levels (R_0). Values shown are expressed as means ± SE (WT, $n = 6$ mice; PGC-1α OE, $n = 4$ mice). #Significant difference ($P < 0.05$) between WT and PGC-1α OE. *Significantly different ($P < 0.05$) from initial level for each condition.

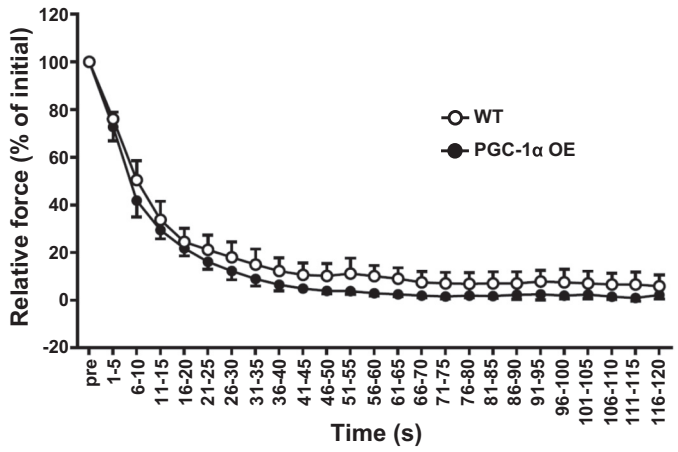

Fig. 2. Relative force profile during 120-s muscle contractions in tibialis anterior muscles from WT and PGC-1α OE mice. Values are means ± SE.

Fig. 1). Thereafter, $[Ca^{2+}]_i$ in PGC-1α OE returned to resting baseline within 150 s. In marked contrast, $[Ca^{2+}]_i$ in WT remained elevated for the entire recovery period (6 ± 1% at 450 s, $P < 0.05$; Fig. 1).

There were no differences in maximal isometric force of TA muscles for PGC-1α OE compared with WT mice (PGC-1α OE, 241.4 ± 19.1 mN; WT, 233.8 ± 18.0 mN, $P > 0.05$). Figure 2 shows the profiles of relative tetanic force production over the 120-s tetanic contractions. There was no difference in force attenuation during this contraction protocol between WT and PGC-1α OE mice.

$[Ca^{2+}]_i$ Regulation During Pharmacological Inhibition of SR and Mitochondrial Function in Resting Muscle

Inhibition of SR Ca^{2+} reuptake with thapsigargin induced a progressive increase in $[Ca^{2+}]_i$ in WT muscles that was markedly attenuated in PGC-1α OE (Figs. 3 and 4, 2 columns on *left*). For instance, in PGC-1α OE muscles, there was no discernible increase in $[Ca^{2+}]_i$ after 30 min. Moreover, after 450 s the $[Ca^{2+}]_i$ increase above initial baseline was significantly higher in WT than PGC-1α OE (i.e., 8.6 vs. 0.6%, $P < 0.05$). FCCP-induced blockade of mitochondrial Ca^{2+} sequestration accelerated the $[Ca^{2+}]_i$ increase in PGC-1α OE muscles and largely removed the greater $[Ca^{2+}]_i$ control evidenced in the PGC-1α OE muscles.

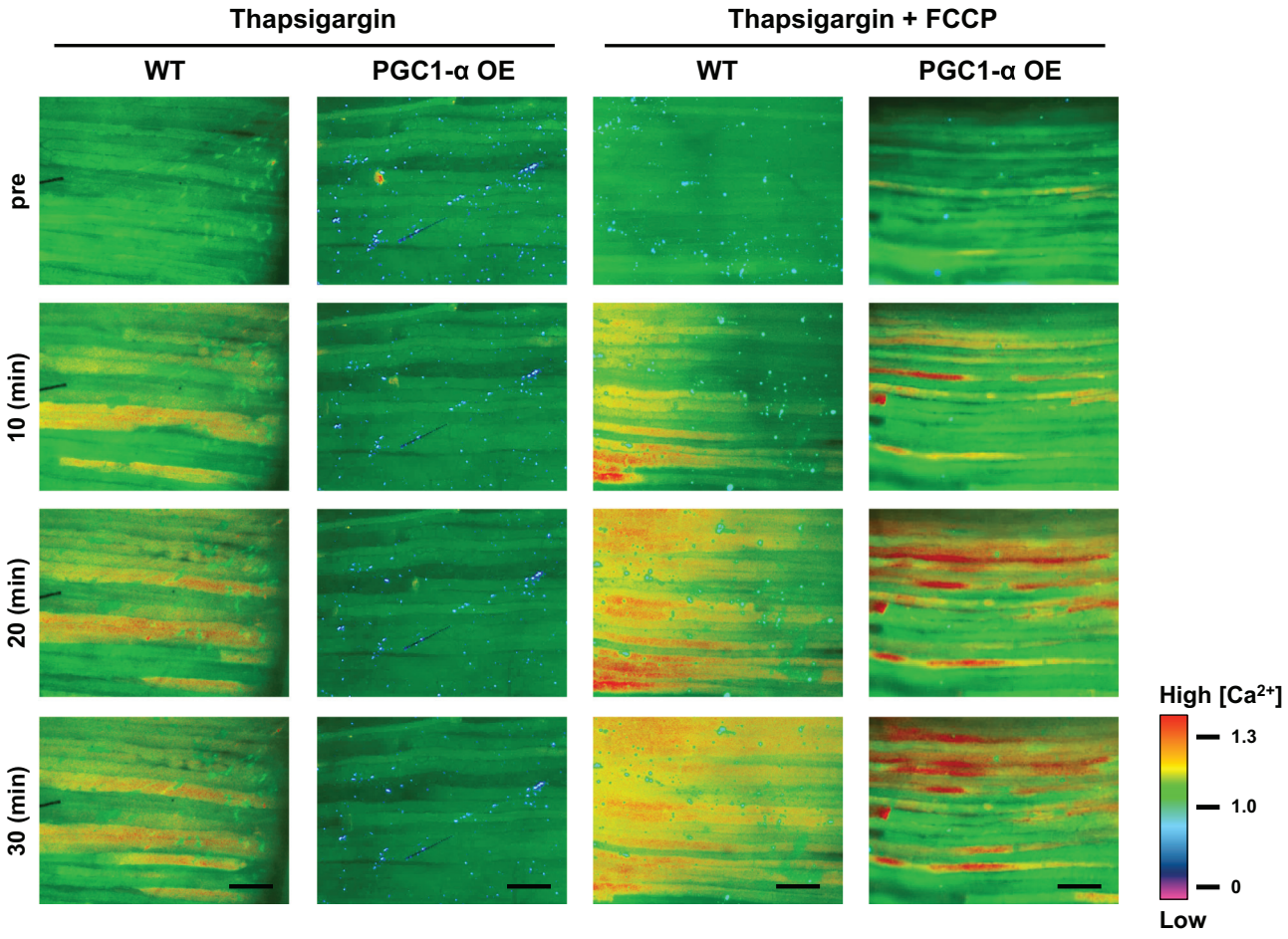

Fig. 3. Typical example of changes in $[Ca^{2+}]_i$ after prolonged exposure to thapsigargin [sarcoplasmic reticulum (SR) Ca^{2+} uptake inhibitor] and carbonyl cyanide-*4*-(trifluoromethoxy) phenylhydrazone (FCCP; mitochondrial Ca^{2+} uptake inhibitor) in WT and PGC-1α OE mice. Scale bar = 200 μm. Note in the two columns on *left* that increased $[Ca^{2+}]_i$ is not discernible at 30 min with SR-inhibition (thapsigargin) PGC-1α OE muscle compared with large increases at 10 min in WT.

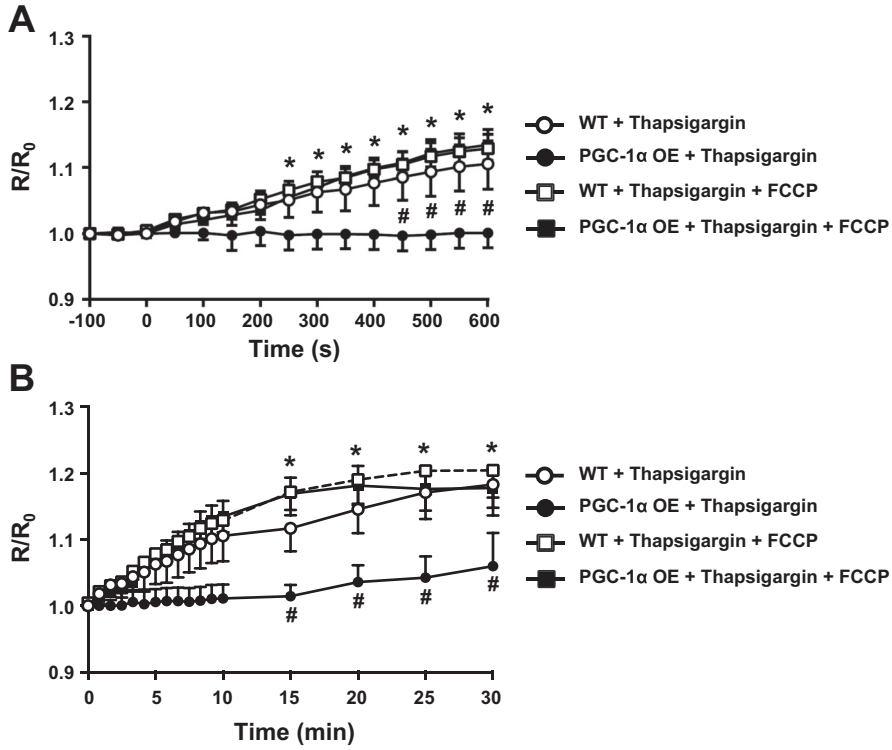

Fig. 4. Effect of thapsigargin and FCCP in tibialis anterior muscle in vivo on $[Ca^{2+}]_i$. Thapsigargin is a high-affinity specific inhibitor of the sarcoplasmic reticulum Ca^{2+}-ATPase. FCCP is an oxidative phosphorylation uncoupler in mitochondria and acts to block mitochondrial Ca^{2+} uptake after 5 min incubation in 10 μM FCCP. *A*: 600 s (i.e., 10 min) of exposure to thapsigargin. *B*: 40 min of exposure to thapsigargin. Fluorescence was measured, and ratiometrically quantified data were graphed as changes from precondition (i.e., −100 s) levels (R_0). The statistical treatment is shown in the RESULTS. Values shown are expressed as means ± SE (WT + thapsigargin, $n = 7$; WT + thapsigargin + FCCP, $n = 6$; PGC-1α OE + thapsigargin, $n = 6$; PGC-1α OE + thapsigargin + FCCP, $n = 7$). #Significant difference ($P < 0.05$) vs. WT + thapsigarigin. *Significantly different ($P < 0.05$) from initial level for each condition (WT + thapsigargin, WT + thapsigargin + FCCP, and PGC-1α OE + thapsigargin + FCCP).

Mitochondrial Ca^{2+} Uptake Following 120-s Tetanic Contractions and During Pharmacological Inhibition of SR

Mitochondrial Ca^{2+} levels following 120-s tetanic contractions were increased ~30% in PGC-1α OE ($P < 0.05$ vs. baseline) and ~20% in WT ($P < 0.05$; Fig. 5). Thereafter, both PGC-1α OE and WT muscle mitochondrial Ca^{2+} levels decreased to baseline levels in 350–450 s. Figure 6 shows the mitochondria Ca^{2+} levels during pharmacological inhibition of SR. In WT muscle, mitochondria Ca^{2+} levels progressively decreased below baseline levels. This response may be caused by Rhod 2 fluorescence degradation, since it is a single-wavelength characteristic. However, in marked contrast, mitochondria Ca^{2+} levels in PGC-1α OE did not decrease but rather were increased by pharmacological inhibition of SR to a peak of 7.8 ± 0.6% at 600 s. These data support that PGC-1α OE increases mitochondrial $[Ca^{2+}]$ levels compared with WT.

Quantitative Analysis of Electron Microscopy in PGC-1α OE

The total number and size of mitochondrial cross sections (and thus mitochondrial volume density) were significantly increased in PGC-1α OE compared with WT (Fig. 7, *F* and *G*). In addition, the minimum distance between sites of Ca^{2+} release from SR (i.e., RyRs) and mitochondrial outer membrane was reduced from 193.2 ± 22.9 to 76.7 ± 7.9 nm in PGC-1α OE vs. WT ($P < 0.05$, Fig. 7*H*).

Ca^{2+} Regulatory Proteins in SR and Mitochondria in PGC-1α OE

Figure 8 demonstrates the differential effects of PGC-1α OE on critical proteins involved in skeletal muscle Ca^{2+} regulation (RyR, CSQ, SERCA1, PV, Mfn1, Mfn2, MCU, and COX IV). Notice that there was a dichotomy of responses between SR and mitochondrial Ca^{2+} uptake-related proteins. Specifically, there were no differences in RyR and CSQ expression levels between PGC-1α OE and WT, whereas PV (soluble SR Ca^{2+}-binding protein) and SERCA1 (SR Ca^{2+}-ATPase) decreased in PGC-1α OE (PV, −37.4%; SERCA1, −46.3%, both $P < 0.05$). In contrast, mitochondrial-related proteins (Mfn1, Mfn2, MCU, and Cox IV) were increased in PGC-1α OE compared with WT (Mfn1, +63.0%; Mfn2, +48.6%; MCU +46.7%; Cox IV, +51.0%, $P < 0.05$).

DISCUSSION

The present investigation provides original and compelling support for the mitochondria as a major site for Ca^{2+} sequestration and therefore $[Ca^{2+}]_i$ regulation in skeletal muscle at rest and during recovery from fatiguing tetanic contractions. Specifically: *1*) increased mitochondrial function in PGC-1α OE muscles was associated with accelerated restoration of baseline precontraction $[Ca^{2+}]_i$ following contractions. *2*) PGC-1α OE provided substantial protection against $[Ca^{2+}]_i$ dysregulation in thapsigargin-induced inhibition of SR Ca^{2+} sequestration in resting muscle. This protection (i.e., WT − PGC-1α OE difference) was largely abolished by FCCP-induced mitochondrial dysfunction. *3*) PGC-1α OE showed significantly increased mitochondrial $[Ca^{2+}]$ following contraction and pharmacological inhibition of SR. *4*) PGC-1α OE induced a selective upregulation of mitochondrial Ca^{2+} sequestration-related proteins (i.e., Mfn1, Mfn2, and MCU) while their counterparts in the SR were either unchanged (RyR and CSQ) or downregulated (SERCA1 and PV). These data support that mitochondrial Ca^{2+} uptake may be dependent on mitochondrial volume density and the proximity of the mitochondrial reticulum to the SR.

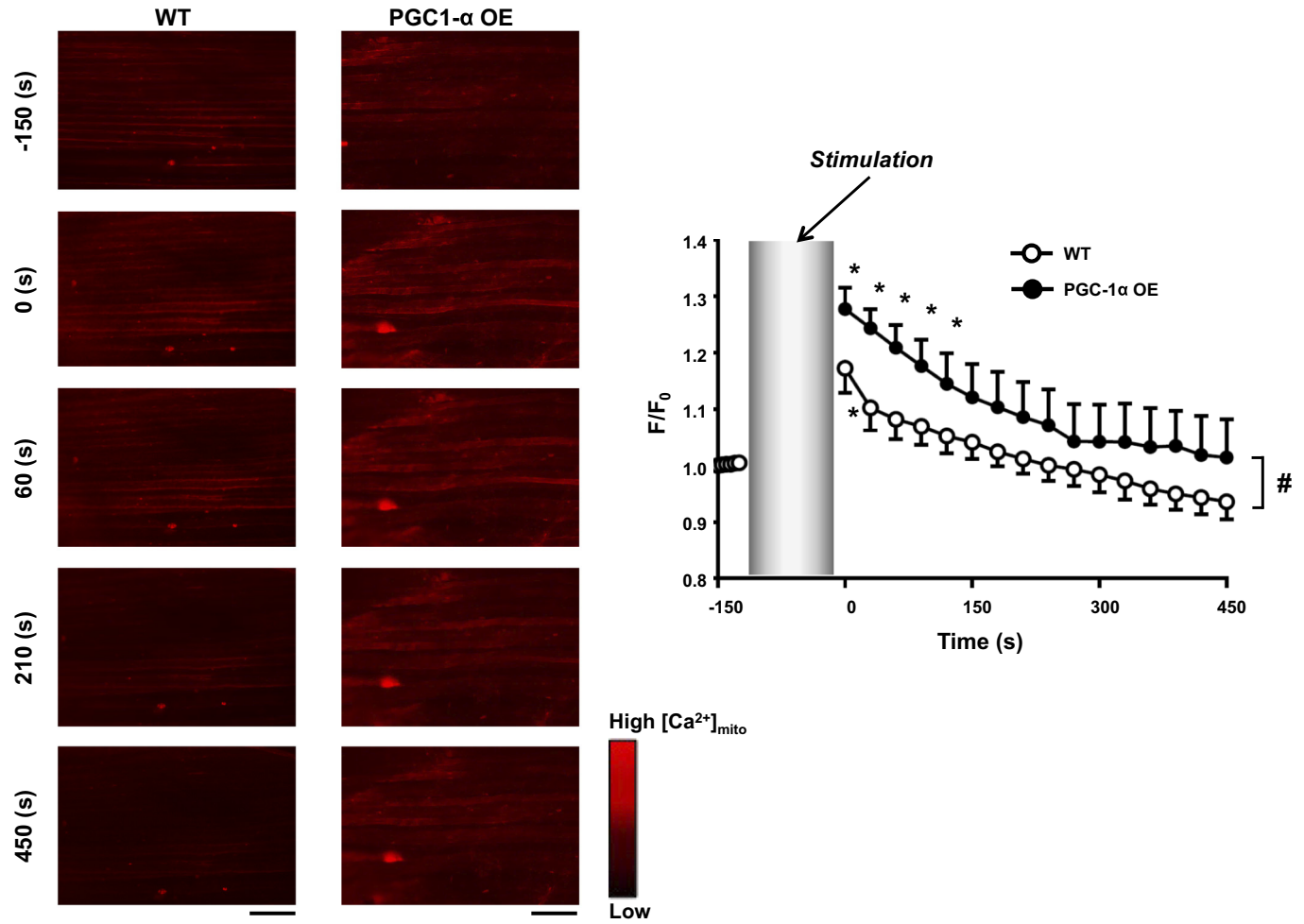

Fig. 5. In vivo mitochondrial Ca^{2+} concentration ($[Ca^{2+}]_{mito}$) profiles following 120-s contractions for tibialis anterior muscles from WT and PGC-1α OE mice. *Left*, Rhod-2 fluorescence images were captured continuously with no delay following contraction. Bar = 200 μm. *Right*, fluorescence was measured before contraction and continuously for 450 s of recovery and ratiometrically quantified data were graphed as changes from baseline levels (F_0). Values shown are expressed as means ± SE (WT, $n = 4$; PGC-1α OE, $n = 4$). #Significant difference ($P < 0.05$) between WT and PGC-1α OE at all time points. *Significantly different ($P < 0.05$) from initial level for each condition.

Morphological Properties and Oxidative Enzyme Activity of TA Muscle in PGC1-α OE Mice

In the mouse TA muscle, the superficial and deep regions have pronounced morphological and functional differences in muscle fiber types and oxidative capacity (8). The superficial region, which constitutes the measurement site for Ca^{2+} imaging, herein consists predominantly of low oxidative fast-twitch fibers (IIx and IIb; oxidative/glycolytic fibers in an ~1:3 ratio) in WT mice. We (44) and others (4) have demonstrated increased proportions of oxidative fibers and a concomitant reduction of glycolytic fibers in PGC-1α OE transgenic mice (similar to muscle creatine kinase-PGC-1α-a transgenic mice). Our results demonstrated that muscle-specific overexpression of PGC-1α OE increased SDH activity levels in both the superficial and deep TA regions in conjunction with the aforementioned shift toward a greater fast-twitch oxidative fiber (MHC type IIx) composition (Table 1). Notice also that, although the SDH activity of the IIx fibers was not different between WT and PGC-1α OE, the substantial population of fibers undergoing IIb→IIx conversion (~34% in the superficial region) must have almost doubled their SDH activity to assume that normally found in IIx fibers. In addition, there was ~40–50% increase in IIb oxidative capacity in the superficial region. Together these data demonstrate that the PGC-1α OE condition drove a substantive increase in mitochondrial volume density and function in the region examined by intravital microscopy.

$[Ca^{2+}]_i$ Buffering and Muscle Contractile Performance in PGC-1α OE Mice

Previous studies indicated that the PGC-1α OE model decreased fatigability during ex vivo (11, 31, 46) and in vivo repeated tetanic contractions (25). However, in the present investigation as previously (18), the continuous contraction protocol (i.e., no relaxation) exhibited a precipitous decrease in force to <10% initial levels without a difference between WT and PGC-1α OE. For the present investigation, the crucial aspect of this contraction protocol is that it provides a significant challenge to $[Ca^{2+}]_i$ homeostasis in murine muscles. Thus, tetanic contractions elevate mitochondrial and also cytosolic $[Ca^{2+}]$ in intact mouse fast (39)- but not slow [soleus (10)]-twitch muscle fibers.

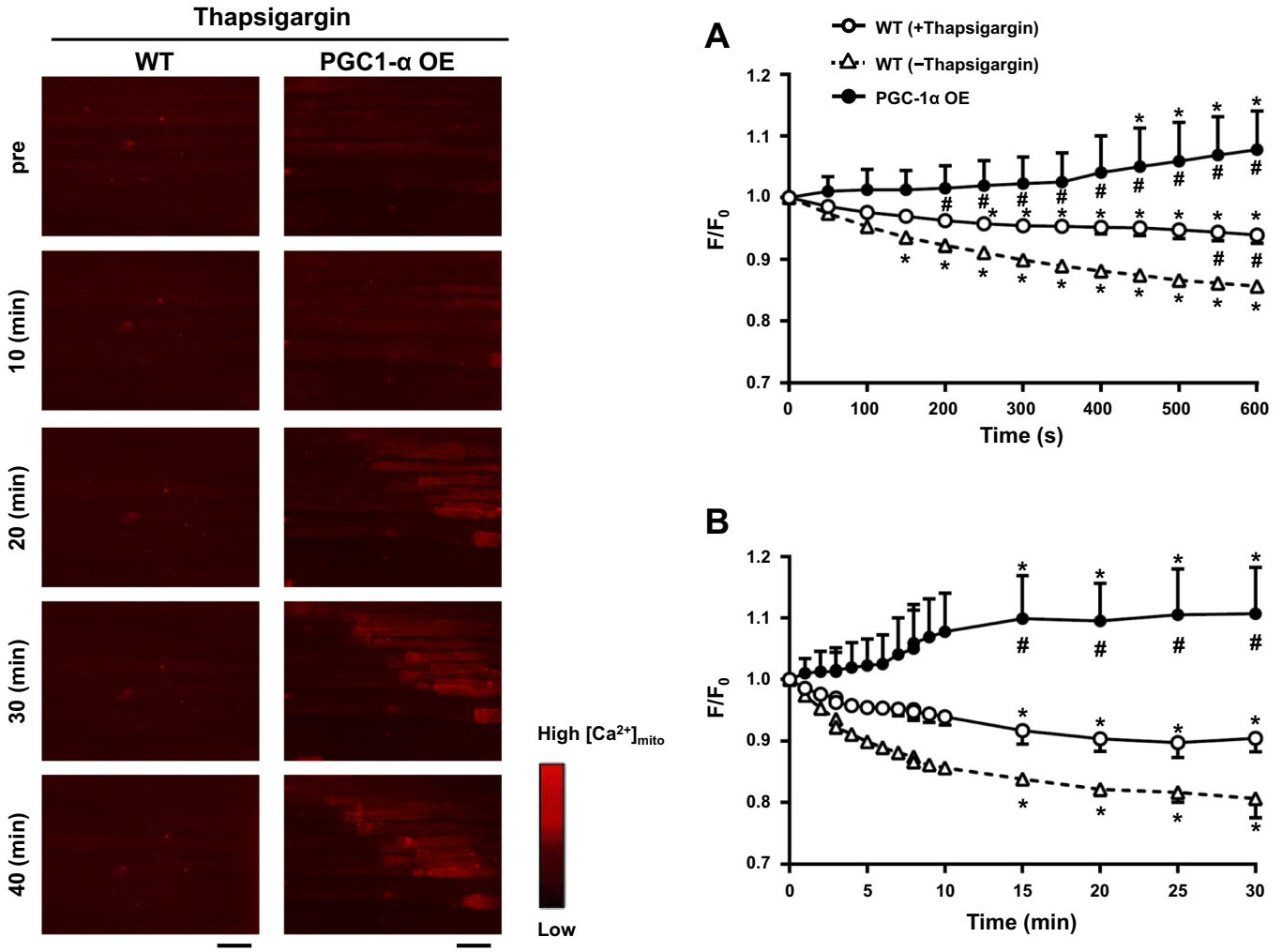

Fig. 6. Effect of thapsigargin in tibialis anterior muscle in vivo on $[Ca^{2+}]_{mito}$. *A*: 600 s (i.e., 10 min) of exposure to thapsigargin. *B*: 40 min of exposure to thapsigargin. Fluorescence was measured, and ratiometrically quantified data were graphed as changes from precondition (i.e., −100 s) levels (F_0). The statistical treatment is shown in the RESULTS. Values shown are expressed as means ± SE (WT + thapsigargin, $n = 7$; WT − thapsigargin, $n = 5$; PGC-1α OE, $n = 5$). #Significant difference ($P < 0.05$) vs. WT − thapsigargin. *Significantly different ($P < 0.05$) from initial level for each condition.

Within skeletal muscle fibers, the mitochondrial reticulum is located adjacent to the SR and close to Ca^{2+} release units (9), supporting that mitochondria and SR may function in a complementary fashion to regulate $[Ca^{2+}]_i$ dynamics. That loss of connectivity of the mitochondria compromises mitochondrial Ca^{2+}-buffering capacity in skeletal myotubes supports this cooperativity (17) as does the cellular Ca^{2+} handling and contractile impairments induced in models of mitochondrial dysfunction such as *Tfam* knockout and mitochondrial DNA mutated mice (6, 47). Thus, the present association between enhanced mitochondrial function in PGC-1α OE and improved $[Ca^{2+}]_i$ homeostasis following a fatiguing tetanic contraction adds further strength to the contention that the mitochondria play an important role in $[Ca^{2+}]_i$ regulation.

In isolated mouse flexor digitorum brevis (FDB) muscle fibers, FCCP effectively poisons the mitochondria uncoupling oxidative phosphorylation and abolishes the mitochondrial potential, which leads to a reduced Ca^{2+} transient amplitude upon electrical stimulation (12). Moreover, FCCP significantly reduces the mitochondrial $[Ca^{2+}]$ increase after repeated tetanic contractions in soleus (10), FDB (1) and *Xenopus* lumbrical (29) skeletal muscle fibers. As expected from the above, Figs. 3 and 4 herein demonstrate that the increased Ca^{2+} buffering conferred to the PGC-1α OE mice was removed by FCCP. Collectively, these investigations support that intracellular $[Ca^{2+}]_i$ regulation in quiescent and contracting fast-twitch skeletal muscle is dependent, in part, on mitochondrial Ca^{2+} sequestration. In this investigation, we followed changes in mitochondrial Ca^{2+} levels using Rhod 2-AM fluorescence to measure mitochondrial $[Ca^{2+}]$. Interestingly, mitochondrial $[Ca^{2+}]$ increased more in PGC-1α OE than WT mice following contractions and during inhibition of the SR Ca^{2+} pump by thapsigargin (Figs. 5 and 6). As mentioned above, these data support that PGC-1α OE contributes to intracellular Ca^{2+} homeostasis by upregulation of mitochondrial Ca^{2+} uptake. It is pertinent that excessively increased mitochondrial $[Ca^{2+}]$ may trigger cell damage and mitochondrial apoptosis (6). Conversely, physiologically stimulated cytosolic Ca^{2+} transients elevate mitochondrial Ca^{2+} levels in vivo in healthy mammalian muscle (40). To our knowledge, the present investigation is the first to demonstrate that mitochondrial $[Ca^{2+}]$ uptake is essential for intracellular Ca^{2+} homeostasis under in vivo conditions.

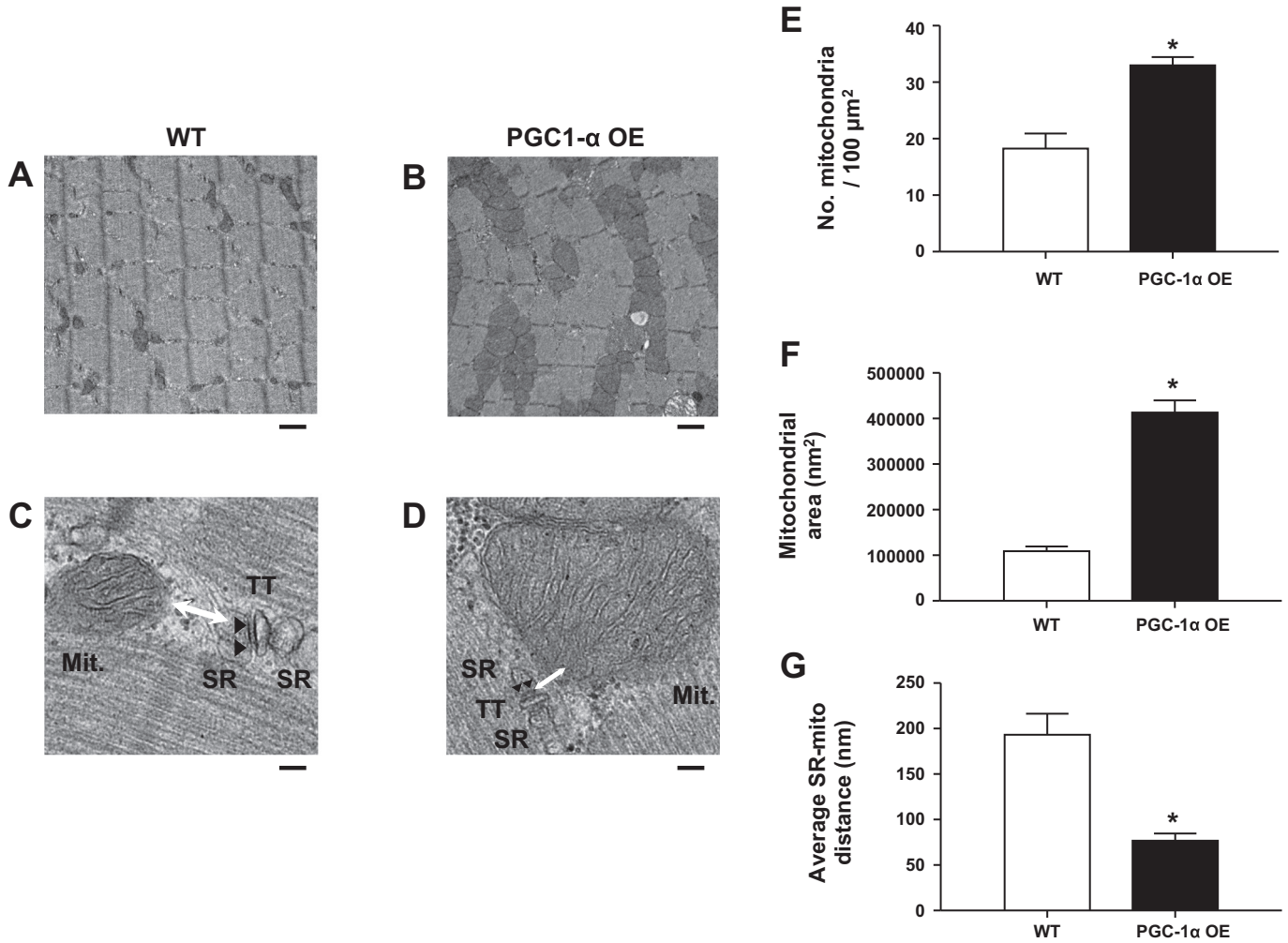

Fig. 7. Electron microscopy analysis of tibialis anterior muscle in WT and PGC-1α OE mice. *Left*, typical images of WT (*A*, *C*, and *E*) and PGC-1α OE (*B* and *D*). Scale bars represent 1 μm (*A* and *B*), 100 nm (*C* and *D*), or 200 nm (*E*). *Right*, quantitative analysis of electron microscopy. Total number of mitochondrial profiles (*F*), individual mitochondria area (*G*,) and distance between SR and mitochondrial outer membrane (*H*). TT, transverse tubular (arrowheads); Mit, individual mitochondria). Values shown are expressed as means ± SE (sample is 80–120 pictures/10 fibers for 3 animals). *Significant difference ($P < 0.05$) between WT and PGC-1α OE.

Mechanisms for Enhanced Mitochondrial Ca^{2+} Uptake in PGC-1α OE Mice

Ca^{2+} buffering protein PV and SERCA protein content decreased in PGC-1α OE mice compared with WT (Fig. 8). PV is a soluble Ca^{2+}-binding protein and highly expressed in mammalian fast-twitch muscle fibers (13, 38), and its absence or overexpression negatively impacts mitochondrial function. For instance, PV knockout mice display prolonged Ca^{2+} transients and cease to regulate mitochondrial volumes, whereas PV overexpression decreases SDH activity in homogenates from slow-twitch fibers such that PV protein content correlates inversely ($r = -0.975$) with SDH activity (14). Accordingly, as evidenced in Table 1 and Fig. 6 herein, SDH activity in IIb muscle fibers was increased in the face of decreased PV content in PGC-1 OE muscles.

SERCA1 protein is coexpressed with fast type II MHC (45), and therefore its expression demonstrates a stratification across fiber types. For example, in rat gastrocnemius muscle, Ca^{2+} pump content decreases from fast glycolytic > fast oxidative glycolytic > slow oxidative types (28). Thus, alterations in fiber-type composition and/or oxidative capacity, consequent to exercise training, for example, impact SERCA1 protein expression (21). Accordingly, in the present investigation, it was expected and found that, with the MHC type II fiber shifts from IIb (glycolytic fibers) to IIx (fast oxidative fibers) in TA muscles of PGC-1α OE mice, the SERCA1 protein expression was decreased (Table 1 and Fig. 8).

Herein we confirmed by electron microscopy that mitochondrial volume density was increased substantially in PGC-1α OE (Fig. 7) mice, which is also associated with enhanced exercise capacity (25, 44). These findings are consistent with the elevated SDH activity and mitochondrial marker proteins in the PGC-1α OE muscles (Table 1 and Fig. 8).

Mfn isoform protein (Mfn1/2) forms electron-dense tethers that bridge the outer mitochondrial membrane to that region of the SR that is in close proximity to the site of Ca^{2+} release. In cardiomyocytes, Mfn2-mediated mitochondrial SR tethering facilitates Ca^{2+} cross talk (15), and it is known that genetic ablation of Mfn2 creates dysfunctional mitochondria-endoplasmic reticulum interactions and increases peak ATP-stimulated

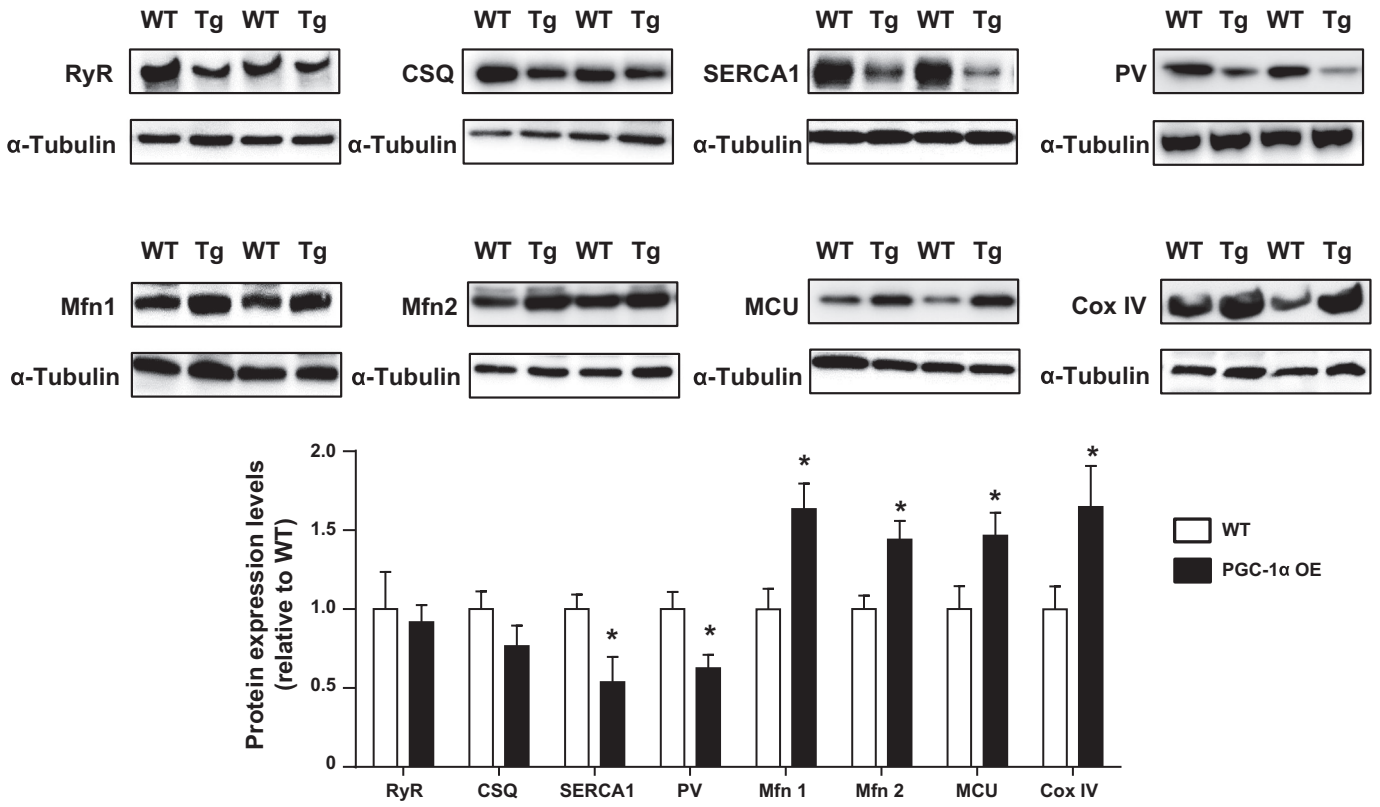

Fig. 8. Expression levels of intracellular Ca^{2+} regulation proteins in WT and PGC-1α OE mice. *Top*, representative Western blot showing ryanodine receptor (RyR), CSQ, SR Ca^{2+}-ATPase (SERCA1), parvalbumin (PV), Mfn1, Mfn2, mitochondrial Ca^{2+} uniporter (MCU), and cytochrome *c* oxidase subunit 4 (COX IV) proteins. PGC-1α OE designated as the "Tg". *Bottom*, protein expression levels were normalized to WT. *Significant difference between WT and PGC-1α OE ($P < 0.05$). Values are means ± SE ($n = 6$–7).

mitochondrial [Ca^{2+}] (22). In skeletal muscle, mitochondrial fusion based on Mfn1 is a key supporter of excitation-contraction coupling in skeletal myotubes (17). In addition, mitochondrial Ca^{2+} uptake is impaired in acute electroporated Mfn2 knockdown mice after tetanic contractions in the absence of changes in Ca^{2+}-regulated proteins (1). In the present investigation, Mfn1 and Mfn2 protein expression levels were higher in PGC-1α OE compared with WT muscles (Fig. 8).

The inner mitochondrial membrane is impermeable to ions, and Ca^{2+} uptake therefore occurs through the MCU (5, 27). The MCU, which binds Ca^{2+} with a high affinity and is effective for promoting Ca^{2+} uptake in energized mitochondria, even at low cytoplasmic concentrations, is therefore believed to play a key role in mitochondrial Ca^{2+} handling. Indeed, mitochondria from MCU knockout mice are unable to rapidly uptake Ca^{2+} and display exercise intolerance that may also relate to changes in pyruvate dehydrogenase phosphorylation and activity (37). In humans, patients with MICU1 (MCU regulator) mutations exhibit lower mitochondrial Ca^{2+} uptake, leading to increased cytosolic Ca^{2+} and profound muscle weakness (32). In contrast, MCU overexpression enhances intracellular Ca^{2+} buffering in ex vivo FDB muscle fibers. Herein MCU protein content significantly increased in PGC-1α OE compared with WT (Fig. 8; $P < 0.05$). It is pertinent that MCU regulates skeletal muscle hypertrophy and atrophy via PGC-1α4 and IGF-I-protein kinase B hypertrophic pathway regulation (33), and either this or the IIb→IIx interconversion has likely contributed to the hypertrophy present in the superficial IIx fibers (Table 1). In addition, Mammucari and colleagues (33) found that MCU regulates mitochondrial volume and may cause proliferation and distortion of cristae.

SR-mitochondrial Ca^{2+} cross talk is thought to play an important role in the Ca^{2+} transients found in mammalian skeletal muscle and is intrinsic to skeletal muscle intracellular Ca^{2+} homeostasis (39). It is pertinent, therefore, that the RyRs were in far closer proximity to the mitochondrial outer membrane in PGC-1α OE than WT muscles (Fig. 7). Our WT values (193 nm) for RyR-mitochondrial outer membrane distance are within the range reported previously in the mouse FDB [i.e., 100–200 nm (9)] and far longer than in our PGC-1α OE muscles (77 nm). It is possible that this anatomical closeness is important for the upregulation of intracellular Ca^{2+} homeostasis in PGC-1α OE muscles.

Experimental Limitations

Initially, during pilot experiments, we attempted to make our battery of measurements during contractions under MCU inhibition, but the technical limitations in the in vivo model proved intractable. Also, because of muscle movement (a constant challenge during intravital microscopy), it was not possible to establish the resolution and clarity necessary for confidence in the Ca^{2+} dynamics during the contraction itself. Changing the basic design of the experimental system to attempt this would have compromised other sentinel measurements. In addition, although it is expected that time-to-twitch

peak tension would be delayed in PGC-1α OE mice (26), our tetanic contraction model precluded this measurement.

Perspectives and Significance

Whereas the exact role of mitochondrial Ca^{2+} handling physiologically remains to be established, enhanced PGC-1α expression (PGC-1α OE) increases Ca^{2+}-buffering capacity and homeostasis in mouse fast-twitch tibialis anterior muscle at rest and following fatiguing tetanic contractions. Because the mitochondria constitute a crucial site for $[Ca^{2+}]_i$ regulation, augmented mitochondrial structure and function presumably underlie this effect. This contention is supported by PGC-1α OE muscles evincing increased Ca^{2+} uptake potential via upregulated Mfn1, Mfn2, and MCU proteins that improve $[Ca^{2+}]_i$ homeostasis independent from SR function. Augmenting mitochondrial biogenesis via overexpression of PGC-1α might be a useful strategy from the perspective of Ca^{2+} homeostasis and energy metabolism, and this may constitute a putative therapeutic approach for skeletal muscle dysfunction associated with chronic heart failure, diabetes, and/or reduced exercise capacity that attends physiological aging.

ACKNOWLEDGMENTS

We thank members of the Laboratory of Morphology and Image Analysis, Biomedical Research Center, Juntendo University Graduate School of Medicine for technical assistance. We acknowledge T. Horikawa for technical assistance with mouse breeding.

GRANTS

This work was supported in part by the Japan Society for the Promotion of Science KAKENHI Grants 22300221, 23650403, and 25560335, the Yamaha Motor Foundation for Sports, The Uehara Memorial Foundation, and the Sasakawa Scientific Research Grant from The Japan Science Society.

DISCLOSURES

No conflicts of interest, financial or otherwise, are declared by the authors.

AUTHOR CONTRIBUTIONS

H.E., S.M., D.C.P., and Y.K. conceived and designed research; H.E., S.M., N.S., K.H., and Y.K. performed experiments; H.E., D.C.P., and Y.K. analyzed data; H.E., S.M., D.C.P., and Y.K. interpreted results of experiments; H.E. and Y.K. prepared figures; H.E., D.C.P., and Y.K. drafted manuscript; H.E., S.M., N.S., K.H., D.C.P., and Y.K. approved final version of manuscript.

REFERENCES

1. **Ainbinder A, Boncompagni S, Protasi F, Dirksen RT.** Role of Mitofusin-2 in mitochondrial localization and calcium uptake in skeletal muscle. *Cell Calcium* 57: 14–24, 2015. doi:10.1016/j.ceca.2014.11.002.
2. **Allen DG, Lamb GD, Westerblad H.** Skeletal muscle fatigue: cellular mechanisms. *Physiol Rev* 88: 287–332, 2008. doi:10.1152/physrev.00015.2007.
3. **Arany Z, Foo SY, Ma Y, Ruas JL, Bommi-Reddy A, Girnun G, Cooper M, Laznik D, Chinsomboon J, Rangwala SM, Baek KH, Rosenzweig A, Spiegelman BM.** HIF-independent regulation of VEGF and angiogenesis by the transcriptional coactivator PGC-1alpha. *Nature* 451: 1008–1012, 2008. doi:10.1038/nature06613.
4. **Arany Z, Lebrasseur N, Morris C, Smith E, Yang W, Ma Y, Chin S, Spiegelman BM.** The transcriptional coactivator PGC-1beta drives the formation of oxidative type IIX fibers in skeletal muscle. *Cell Metab* 5: 35–46, 2007. doi:10.1016/j.cmet.2006.12.003.
5. **Arruda AP, Hotamisligil GS.** Calcium homeostasis and organelle function in the pathogenesis of obesity and diabetes. *Cell Metab* 22: 381–397, 2015. doi:10.1016/j.cmet.2015.06.010.
6. **Aydin J, Andersson DC, Hänninen SL, Wredenberg A, Tavi P, Park CB, Larsson NG, Bruton JD, Westerblad H.** Increased mitochondrial Ca^{2+} and decreased sarcoplasmic reticulum Ca^{2+} in mitochondrial myopathy. *Hum Mol Genet* 18: 278–288, 2009. doi:10.1093/hmg/ddn355.
7. **Barclay CJ, Woledge RC, Curtin NA.** Energy turnover for Ca^{2+} cycling in skeletal muscle. *J Muscle Res Cell Motil* 28: 259–274, 2007. doi:10.1007/s10974-007-9116-7.
8. **Bloemberg D, Quadrilatero J.** Rapid determination of myosin heavy chain expression in rat, mouse, and human skeletal muscle using multicolor immunofluorescence analysis. *PLoS One* 7: e35273, 2012. doi:10.1371/journal.pone.0035273.
9. **Boncompagni S, Rossi AE, Micaroni M, Beznoussenko GV, Polishchuk RS, Dirksen RT, Protasi F.** Mitochondria are linked to calcium stores in striated muscle by developmentally regulated tethering structures. *Mol Biol Cell* 20: 1058–1067, 2009. doi:10.1091/mbc.E08-07-0783.
10. **Bruton J, Tavi P, Aydin J, Westerblad H, Lännergren J.** Mitochondrial and myoplasmic $[Ca^{2+}]$ in single fibres from mouse limb muscles during repeated tetanic contractions. *J Physiol* 551: 179–190, 2003. doi:10.1113/jphysiol.2003.043927.
11. **Calvo JA, Daniels TG, Wang X, Paul A, Lin J, Spiegelman BM, Stevenson SC, Rangwala SM.** Muscle-specific expression of PPAR-gamma coactivator-1alpha improves exercise performance and increases peak oxygen uptake. *J Appl Physiol (1985)* 104: 1304–1312, 2008. doi:10.1152/japplphysiol.01231.2007.
12. **Caputo C, Bolaños P.** Effect of mitochondria poisoning by FCCP on Ca^{2+} signaling in mouse skeletal muscle fibers. *Pflügers Arch* 455: 733–743, 2008. doi:10.1007/s00424-007-0317-0.
13. **Celio MR, Heizmann CW.** Calcium-binding protein parvalbumin is associated with fast contracting muscle fibres. *Nature* 297: 504–506, 1982. doi:10.1038/297504a0.
14. **Chin ER, Grange RW, Viau F, Simard AR, Humphries C, Shelton J, Bassel-Duby R, Williams RS, Michel RN.** Alterations in slow-twitch muscle phenotype in transgenic mice overexpressing the Ca^{2+} buffering protein parvalbumin. *J Physiol* 547: 649–663, 2003. doi:10.1113/jphysiol.2002.024760.
15. **Dorn GW II, Song M, Walsh K.** Functional implications of mitofusin 2-mediated mitochondrial-SR tethering. *J Mol Cell Cardiol* 78: 123–128, 2015. doi:10.1016/j.yjmcc.2014.09.015.
16. **Du GG, Ashley CC, Lea TJ.** Effects of thapsigargin and cyclopiazonic acid on the sarcoplasmic reticulum Ca^{2+} pump of skinned fibres from frog skeletal muscle. *Pflügers Arch* 429: 169–175, 1994. doi:10.1007/BF00374309.
17. **Eisner V, Parra V, Lavandero S, Hidalgo C, Jaimovich E.** Mitochondria fine-tune the slow Ca^{2+} transients induced by electrical stimulation of skeletal myotubes. *Cell Calcium* 48: 358–370, 2010. doi:10.1016/j.ceca.2010.11.001.
18. **Eshima H, Poole DC, Kano Y.** In vivo Ca^{2+} buffering capacity and microvascular oxygen pressures following muscle contractions in diabetic rat skeletal muscles: fiber-type specific effects. *Am J Physiol Regul Integr Comp Physiol* 309: R128–R137, 2015. doi:10.1152/ajpregu.00044.2015.
19. **Eshima H, Poole DC, Kano Y.** In vivo calcium regulation in diabetic skeletal muscle. *Cell Calcium* 56: 381–389, 2014. doi:10.1016/j.ceca.2014.08.008.
20. **Eshima H, Tanaka Y, Sonobe T, Inagaki T, Nakajima T, Poole DC, Kano Y.** In vivo imaging of intracellular Ca^{2+} after muscle contractions and direct Ca^{2+} injection in rat skeletal muscle in diabetes. *Am J Physiol Regul Integr Comp Physiol* 305: R610–R618, 2013. doi:10.1152/ajpregu.00023.2013.
21. **Ferreira JC, Bacurau AV, Bueno CR Jr, Cunha TC, Tanaka LY, Jardim MA, Ramires PR, Brum PC.** Aerobic exercise training improves Ca^{2+} handling and redox status of skeletal muscle in mice. *Exp Biol Med (Maywood)* 235: 497–505, 2010. doi:10.1258/ebm.2009.009165.
22. **Filadi R, Greotti E, Turacchio G, Luini A, Pozzan T, Pizzo P.** Mitofusin 2 ablation increases endoplasmic reticulum-mitochondria coupling. *Proc Natl Acad Sci USA* 112: E2174–E2181, 2015. doi:10.1073/pnas.1504880112.
23. **González Narváez AA, Castillo A.** Ca^{2+} store determines gating of store operated calcium entry in mammalian skeletal muscle. *J Muscle Res Cell Motil* 28: 105–113, 2007. doi:10.1007/s10974-007-9105-x.
24. **Gordon CS, Serino AS, Krause MP, Campbell JE, Cafarelli E, Adegoke OA, Hawke TJ, Riddell MC.** Impaired growth and force production in skeletal muscles of young partially pancreatectomized rats: a model of adolescent type 1 diabetic myopathy? *PLoS One* 5: e14032, 2010. doi:10.1371/journal.pone.0014032.
25. **Kano Y, Miura S, Eshima H, Ezaki O, Poole DC.** The effects of PGC-1α on control of microvascular P_{O_2} kinetics following onset of

muscle contractions. *J Appl Physiol (1985)* 117: 163–170, 2014. doi:10.1152/japplphysiol.00080.2014.

26. **Kim JA, Roy RR, Zhong H, Alaynick WA, Embler E, Jang C, Gomez G, Sonoda T, Evans RM, Edgerton VR.** PPARδ preserves a high resistance to fatigue in the mouse medial gastrocnemius after spinal cord transection. *Muscle Nerve* 53: 287–296, 2016. doi:10.1002/mus.24723.
27. **Kirichok Y, Krapivinsky G, Clapham DE.** The mitochondrial calcium uniporter is a highly selective ion channel. *Nature* 427: 360–364, 2004. doi:10.1038/nature02246.
28. **Krenács T, Molnár E, Dobó E, Dux L.** Fibre typing using sarcoplasmic reticulum Ca^{2+}-ATPase and myoglobin immunohistochemistry in rat gastrocnemius muscle. *Histochem J* 21: 145–155, 1989. doi:10.1007/BF01007489.
29. **Lännergren J, Westerblad H, Bruton JD.** Changes in mitochondrial Ca^{2+} detected with Rhod-2 in single frog and mouse skeletal muscle fibres during and after repeated tetanic contractions. *J Muscle Res Cell Motil* 22: 265–275, 2001. doi:10.1023/A:1012227009544.
30. **Lin J, Handschin C, Spiegelman BM.** Metabolic control through the PGC-1 family of transcription coactivators. *Cell Metab* 1: 361–370, 2005. doi:10.1016/j.cmet.2005.05.004.
31. **Lin J, Wu H, Tarr PT, Zhang CY, Wu Z, Boss O, Michael LF, Puigserver P, Isotani E, Olson EN, Lowell BB, Bassel-Duby R, Spiegelman BM.** Transcriptional co-activator PGC-1 alpha drives the formation of slow-twitch muscle fibres. *Nature* 418: 797–801, 2002. doi:10.1038/nature00904.
32. **Logan CV, Szabadkai G, Sharpe JA, Parry DA, Torelli S, Childs AM, Kriek M, Phadke R, Johnson CA, Roberts NY, Bonthron DT, Pysden KA, Whyte T, Munteanu I, Foley AR, Wheway G, Szymanska K, Natarajan S, Abdelhamed ZA, Morgan JE, Roper H, Santen GW, Niks EH, van der Pol WL, Lindhout D, Raffaello A, De Stefani D, den Dunnen JT, Sun Y, Ginjaar I, Sewry CA, Hurles M, Rizzuto R, Duchen MR, Muntoni F, Sheridan E, Sheridan E; UK10K Consortium.** Loss-of-function mutations in MICU1 cause a brain and muscle disorder linked to primary alterations in mitochondrial calcium signaling. *Nat Genet* 46: 188–193, 2014. doi:10.1038/ng.2851.
33. **Mammucari C, Gherardi G, Zamparo I, Raffaello A, Boncompagni S, Chemello F, Cagnin S, Braga A, Zanin S, Pallafacchina G, Zentilin L, Sandri M, De Stefani D, Protasi F, Lanfranchi G, Rizzuto R.** The mitochondrial calcium uniporter controls skeletal muscle trophism in vivo. *Cell Reports* 10: 1269–1279, 2015. doi:10.1016/j.celrep.2015.01.056.
34. **Miura S, Kai Y, Kamei Y, Ezaki O.** Isoform-specific increases in murine skeletal muscle peroxisome proliferator-activated receptor-gamma coactivator-1alpha (PGC-1alpha) mRNA in response to beta2-adrenergic receptor activation and exercise. *Endocrinology* 149: 4527–4533, 2008. doi:10.1210/en.2008-0466.
35. **Miura S, Kai Y, Ono M, Ezaki O.** Overexpression of peroxisome proliferator-activated receptor gamma coactivator-1alpha down-regulates GLUT4 mRNA in skeletal muscles. *J Biol Chem* 278: 31385–31390, 2003. doi:10.1074/jbc.M304312200.
36. **Olesen J, Kiilerich K, Pilegaard H.** PGC-1alpha-mediated adaptations in skeletal muscle. *Pflügers Arch* 460: 153–162, 2010. doi:10.1007/s00424-010-0834-0.
37. **Pan X, Liu J, Nguyen T, Liu C, Sun J, Teng Y, Fergusson MM, Rovira II, Allen M, Springer DA, Aponte AM, Gucek M, Balaban RS, Murphy E, Finkel T.** The physiological role of mitochondrial calcium revealed by mice lacking the mitochondrial calcium uniporter. *Nat Cell Biol* 15: 1464–1472, 2013. doi:10.1038/ncb2868.
38. **Racay P, Gregory P, Schwaller B.** Parvalbumin deficiency in fast-twitch muscles leads to increased 'slow-twitch type' mitochondria, but does not affect the expression of fiber specific proteins. *FEBS J* 273: 96–108, 2006. doi:10.1111/j.1742-4658.2005.05046.x.
39. **Rossi AE, Boncompagni S, Wei L, Protasi F, Dirksen RT.** Differential impact of mitochondrial positioning on mitochondrial Ca^{2+} uptake and Ca^{2+} spark suppression in skeletal muscle. *Am J Physiol Cell Physiol* 301: C1128–C1139, 2011. doi:10.1152/ajpcell.00194.2011.
40. **Rudolf R, Mongillo M, Magalhães PJ, Pozzan T.** In vivo monitoring of Ca^{2+} uptake into mitochondria of mouse skeletal muscle during contraction. *J Cell Biol* 166: 527–536, 2004. doi:10.1083/jcb.200403102.
41. **Shkryl VM, Shirokova N.** Transfer and tunneling of Ca^{2+} from sarcoplasmic reticulum to mitochondria in skeletal muscle. *J Biol Chem* 281: 1547–1554, 2006. doi:10.1074/jbc.M505024200.
42. **Sonobe T, Inagaki T, Poole DC, Kano Y.** Intracellular calcium accumulation following eccentric contractions in rat skeletal muscle in vivo: role of stretch-activated channels. *Am J Physiol Regul Integr Comp Physiol* 294: R1329–R1337, 2008. doi:10.1152/ajpregu.00815.2007.
43. **Sonobe T, Inagaki T, Sudo M, Poole DC, Kano Y.** Sex differences in intracellular Ca^{2+} accumulation following eccentric contractions of rat skeletal muscle in vivo. *Am J Physiol Regul Integr Comp Physiol* 299: R1006–R1012, 2010. doi:10.1152/ajpregu.00623.2009.
44. **Tadaishi M, Miura S, Kai Y, Kano Y, Oishi Y, Ezaki O.** Skeletal muscle-specific expression of PGC-1α-b, an exercise-responsive isoform, increases exercise capacity and peak oxygen uptake. *PLoS One* 6: e28290, 2011. doi:10.1371/journal.pone.0028290.
45. **Talmadge RJ, Roy RR, Chalmers GR, Edgerton VR.** MHC and sarcoplasmic reticulum protein isoforms in functionally overloaded cat plantaris muscle fibers. *J Appl Physiol (1985)* 80: 1296–1303, 1996.
46. **Wende AR, Schaeffer PJ, Parker GJ, Zechner C, Han DH, Chen MM, Hancock CR, Lehman JJ, Huss JM, McClain DA, Holloszy JO, Kelly DP.** A role for the transcriptional coactivator PGC-1alpha in muscle refueling. *J Biol Chem* 282: 36642–36651, 2007. doi:10.1074/jbc.M707006200.
47. **Yamada T, Ivarsson N, Hernández A, Fahlström A, Cheng AJ, Zhang SJ, Bruton JD, Ulfhake B, Westerblad H.** Impaired mitochondrial respiration and decreased fatigue resistance followed by severe muscle weakness in skeletal muscle of mitochondrial DNA mutator mice. *J Physiol* 590: 6187–6197, 2012. doi:10.1113/jphysiol.2012.240077.
48. **Yan Z, Okutsu M, Akhtar YN, Lira VA.** Regulation of exercise-induced fiber type transformation, mitochondrial biogenesis, and angiogenesis in skeletal muscle. *J Appl Physiol (1985)* 110: 264–274, 2011. doi:10.1152/japplphysiol.00993.2010.